DC Conduction in Butyl Rubber (IIR) Loaded with Carbon Black

A. ABO-HASHEM

Physics Department, Faculty of Science, Ain Shams University, Cairo, Egypt

SYNOPSIS

Current–voltage characteristics of samples of butyl rubber loaded with two different types of carbon black have been studied at different temperatures in the voltage range 10–3 KV. The conduction mechanism was found to follow the conventional band approach followed by the hopping model for isobutylene isoprene rubber (IIR) mixed with 40 phr of fast-extrusion furnace black (FEF) carbon black and the hopping model for IIR mixed with 50 phr of semireinforcing furnace black (SRF) carbon black. © 1992 John Wiley & Sons, Inc.

INTRODUCTION

The electrical conduction process in carbon black–polymer composites is complicated, depending on a large number of parameters: particle size, surface area, surface condition, and dispersion of carbon particles.[1-4] Electrical conduction is essentially explained by a combination of percolation and quantum mechanical tunneling that control the current flow via the carbon particles.[5-7] According to some authors, the interaction between carbon black and polymer plays an important role in the electrical conductivity of these composites.[8]

When current–voltage characteristics of carbon black–polymer composites are studied, for most composites, the current does not vary linearly with applied voltage except at low field.[4,6,9,10] At high fields, it may vary as the square of the applied voltage, and at very high voltage, the current may depend upon higher powers of the voltage depending upon the type of composite. The main reason for this behavior is the charge that accumulates within these composites and, consequently, alters the internal field. The current under these conditions is said to be space-charge limited.

The aim of this work was the investigation of the current–voltage characteristics at different temperatures for isobutylene isoprene rubber (IIR) loaded with two types of carbon black. They differ greatly in their particle size, surface area, and surface conditions of carbon particles. The space-charge limited current is encountered for these composites. Therefore, the wealth of information that is obtained from the space-charge limited current enables us to describe the condition mechanism in these composites by the conventional band model. This mechanism is based upon the interaction between carbon black and IIR.

EXPERIMENTAL

Samples of butyl rubber (IIR) loaded with fast-extrusion furnace black (FEF) and semireinforcing furnace black (SRF) were prepared according to Table I. Table II gives some characteristics of the used blacks. The investigated samples were molded on a two-roll mill, 17 cm in diameter, with working distance of 30 cm, slow roll speed of 24 rev/min, and gear ratio of 1.4. The mixtures were left for at least 24 h before vulcanization. The samples were vulcanized at 150 ± 2°C inside pressure of about 40 kg/cm^2 for 30 min. The samples were shaped in the form of disc of 1.5 cm in diameter and 0.3 cm thick.

The electrodes were silver paste covering the opposite surface of the sample over a circular area of 1 cm in diameter. The samples were thermally aged at 90°C for 35 days to attain reasonable stability. The sample holder consists of two parallel plates of

Journal of Applied Polymer Science, Vol. 45, 1733–1741 (1992)
 CCC 0021-8995/92/101733-09$04.00

Table I The Composition of IIR Samples Containing FEF and SRF Carbon Black

Ingredients	(phr)[a]
IIR	100
Steric acid	2
Zinc oxide	5
Processing oil	10
FEF	40
SRF	50
MBTS[b]	2
PBN[c]	1
Sulphur	2

[a] Parts per hundred parts of rubber by weight.
[b] Dibenzthiaryle disulfide.
[c] Phenyl-β-naphthylamine.

brass of diameter 1 cm. The sample holder is a Teflon stoppered glass tube containing silica gel as a drying agent.

RESULTS

Figures 1 and 2 show the current–voltage (I–V) characteristics on a log–log scale for IIR loaded with 40 FEF and 50 SRF carbon black, respectively, at different temperatures. We find that the conduction is ohmic ($I \propto V$) at low field. At intermediate fields, a square law region ($I \propto V^2$) is obtained, followed by a region $I \propto V^n$ ($n \approx 3$–4 for SRF composite). The current density (J) in the square law region is given by the relation[12–15]

$$J = \frac{9\epsilon\epsilon_0\mu_0 V^2}{8a^3} \quad (1)$$

where μ_0 is the free carrier mobility; ϵ_0, the permittivity of free space; ϵ, the dielectric constant of the sample material ($\epsilon = 17$ for 40 FEF composite and 12 for 50 SRF composite)[16]; and a, the sample thickness.

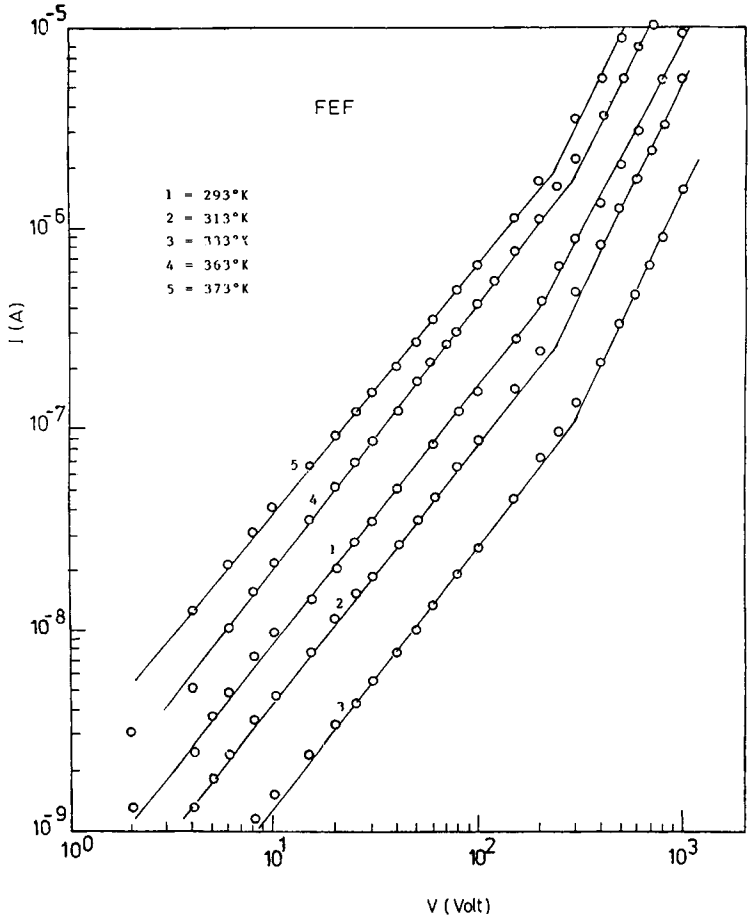

Figure 1 I–V characteristics on log–log scale for the FEF composite.

Table II Characteristics of the Used Carbon Black[11]

Carbon Black	ASTM	Particle Diameter Arithmetic Mean (Å)	Surface Area (m^2/g)	Oil Absorption (cc/g)
FEF	N550	360	55	1.34
SRF	N220	700	28	0.67

Figures 3 and 4 show the plot of current (I) as a function of the square of the applied voltage (V^2) in the square law region for FEF composite at different temperatures. Figure 5 shows the same plot for SRF composite. The (I-V^2) plots fit straight lines at different temperatures for the two composites, indicating the formation of space-charge in these composites. The formation of space-charge is due to the existence of traps within these composites that can occur at particular molecular sites and chain folds.[17] When a trap level exists, the electron mobility is reduced by $1/\theta$, and the effective electron drift mobility (μ_e) in an insulator with traps is, therefore,

$$\mu_e = \mu_0\theta \tag{2}$$

where θ is the trapping factor

$$\theta = N_c/N_t \exp(-E_t/kT) \tag{3}$$

where N_c is the effective density of states in the conduction band and N_t is the shallow trap density at energy E_t below the conduction band edge, k is the Boltzmann constant, and T is the absolute temperature. Therefore, in the trap-square law region, which is our case, the relation between J and V^2 becomes[13,15]

$$J = \frac{9\epsilon,\ \epsilon_0\theta\mu_0 V^2}{8a^3} \tag{4}$$

The free current carrier mobility (μ_0) can be calculated at different temperatures using the experimental value of θ and the slope of (I-V^2) plots for the two composites. Experimentally, θ is the ratio between the current densities at the beginning I_1 and the end I_2 of the trap-square law region.[14] Again, θ is the ratio between the free electron concentration n_0 in the conduction band to the total electron density ($n_0 + n_t$), n_t being the density of the trapped electrons. Thus,

$$I_1/I_2 = \theta = n_0/(n_0 + n_t) \tag{5}$$

Figure 6 shows the variation of the calculated μ_0 with temperature for the two composites. We found that for the FEF composite μ_0 decreases with increasing temperature and reaches a minimum value at 333 K, while for the SRF composite, μ_0 shows an increase with temperature. The behavior of μ_0 with temperature for both composites was identical with that observed for the electrical conductivity (σ) with temperature (in the ohmic region), as illustrated in Figure 7.

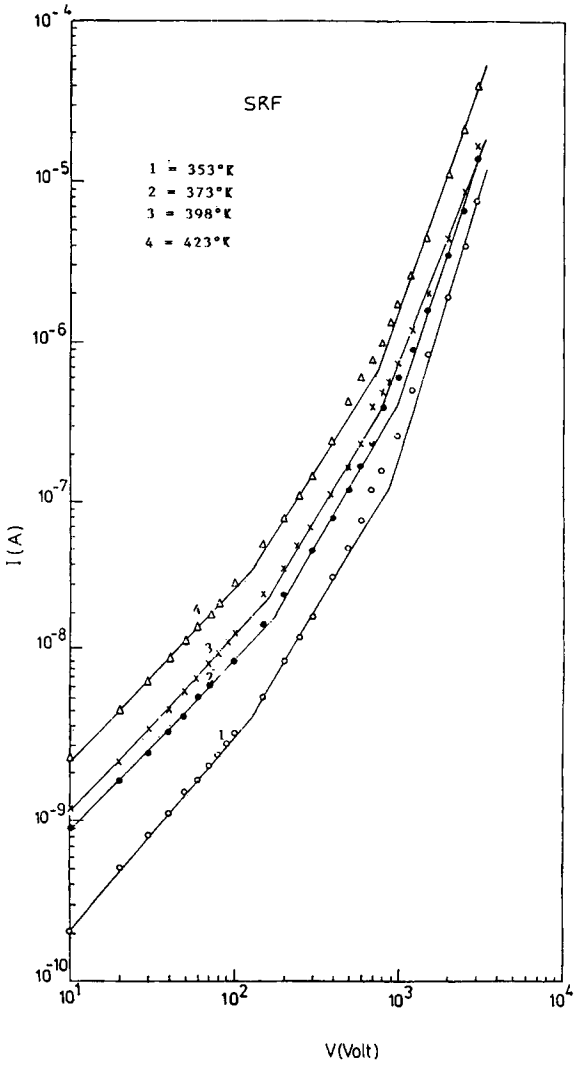

Figure 2 I-V characteristics on log-log scale for the SRF composite.

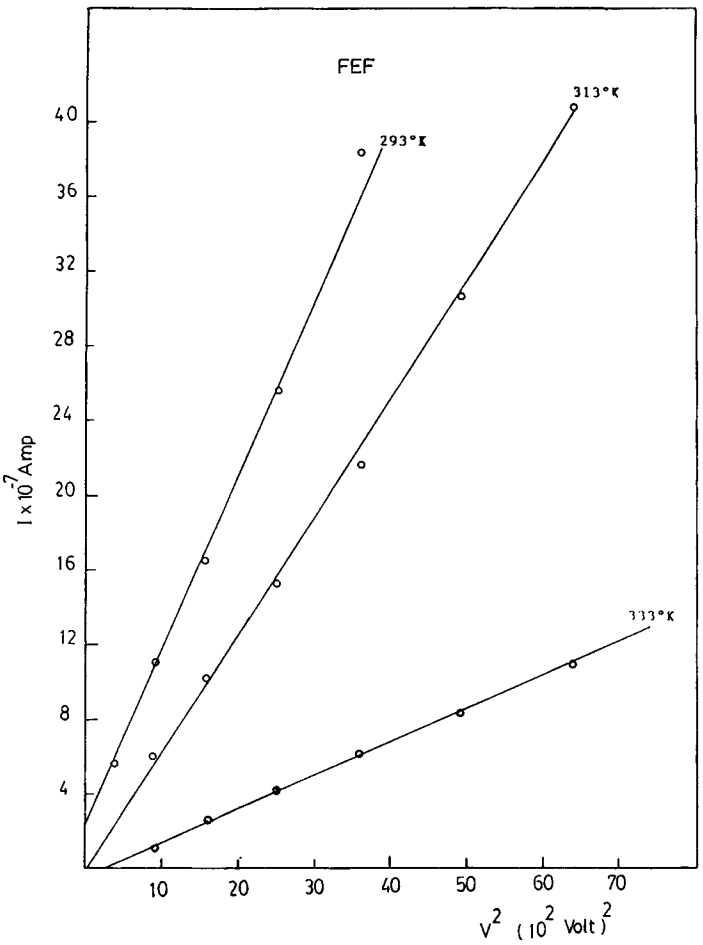

Figure 3 I-V^2 plot for the FEF composite in the square law region at 298, 313, and 333 K.

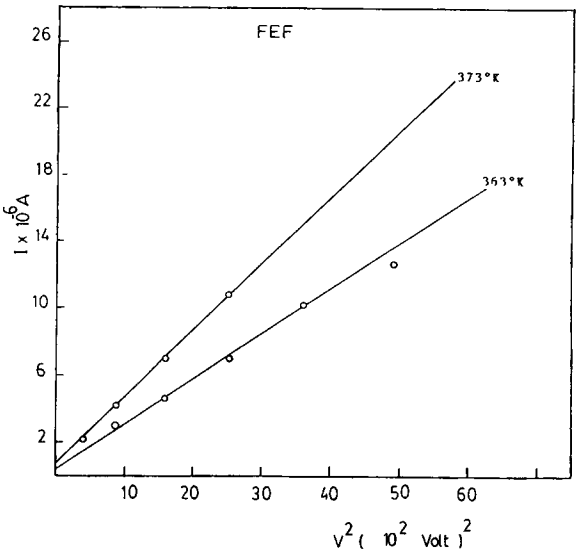

Figure 4 I-V^2 plot for the FEF composite in the square law region at 363 and 373 K.

Using the experimental values of θ at different temperatures in eq. (3), E_t can be determined by plotting log θ against $1/T$. Figure 8 shows such a plot for the two composites. From the slope of both lines, E_t was found to be 0.09 eV for the FEF composite and 0.14 eV for the SRF composite.

The equilibrium concentration of the charge carrier in the conduction band n_0 can also be obtained using the relation[14]

$$n_0 = \left(\frac{\epsilon\epsilon_0\theta}{qa^2}\right)V_{tr} \tag{6}$$

where q is the electron charge and V_{tr} is the voltage at which the transition from the ohmic to square law region takes place. The free carrier density n_0 may be used in eq. (5) to determine the values of n_t, the trap carrier density.

For one type of current carrier, the conductivity is given by

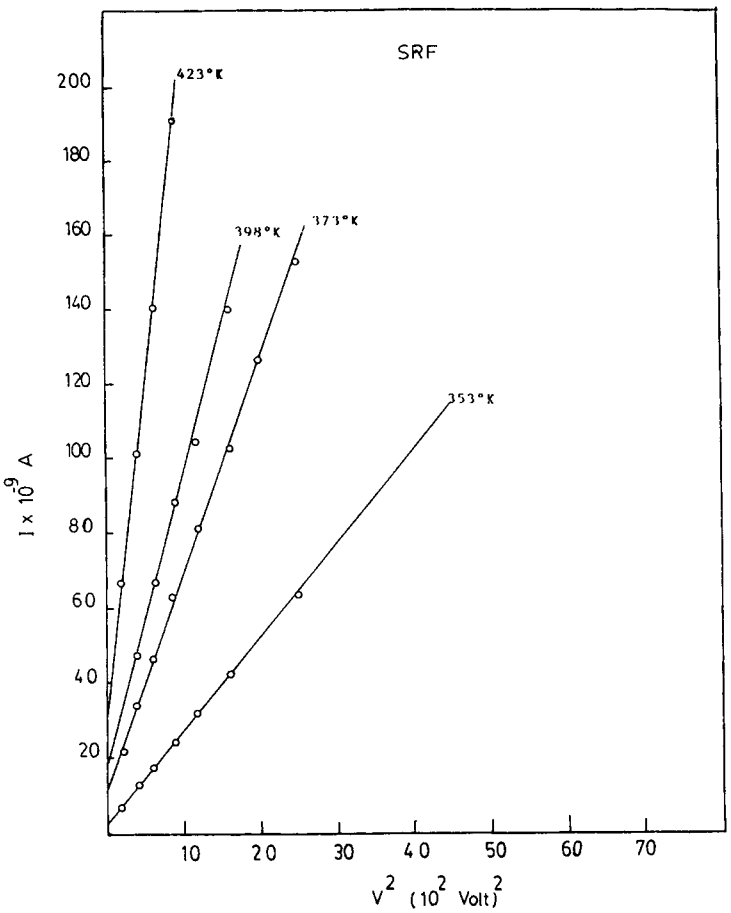

Figure 5 I-V^2 plot for the SRF composite in the square law region at different temperatures.

$$\sigma = qn_0\mu_0 \tag{7}$$

Using the calculated values of n_0 and μ_0 in this equation, we found that the calculated values of σ agreed with the values determined from the ohmic region.

The Fermi level E_f measured from the bottom of the conduction band can be given by

$$n_0 = N_c \exp(-E_f/kT) \tag{8}$$

Figure 9 shows a plot of log n_0 against $1/T$ for the two composites. Comparing this figure with Figure 7, we found that the behavior of n_0 with $1/T$ is the reverse of the $\sigma - 1/T$ plot for the FEF composite and is the same with that of the SRF composite.

Fermi energy can be determined from the slope of log n_0 against $1/T$ (increasing part) for the two composites. The Fermi level E_f was found to be 0.15 eV for the FEF composite and 0.21 eV for the SRF composite. Tables III and IV give the calculated parameters for the FEF and SRF composites.

DISCUSSION

IIR is a crystalline polymer.[18] Polymer crystals are molecular crystal in which the intermolecular interaction is weak, the bands are narrow, and the mobility is low. The electrical conductivity of a crystalline polymer shows a reduction at high field (before breakdown).[19] This reduction was attributed to the narrow band effect. In our case, which is a crystalline polymer (IIR) loaded with carbon black, the reduction in the electrical conductivity at high field was not observed. This may be due to the enhancement of the bandwidth (w) of IIR by mixing with carbon black.

For narrow-band semiconductors, μ is given by the relation

$$\mu = 1.4 \frac{w}{kT} \text{ cm}^2\text{V}^{-1}\text{s}^{-1} \tag{9}$$

where w is the bandwidth. The bandwidth in a crystalline polymer lies between 10^{-2} and 10^{-3} eV.[20] Us-

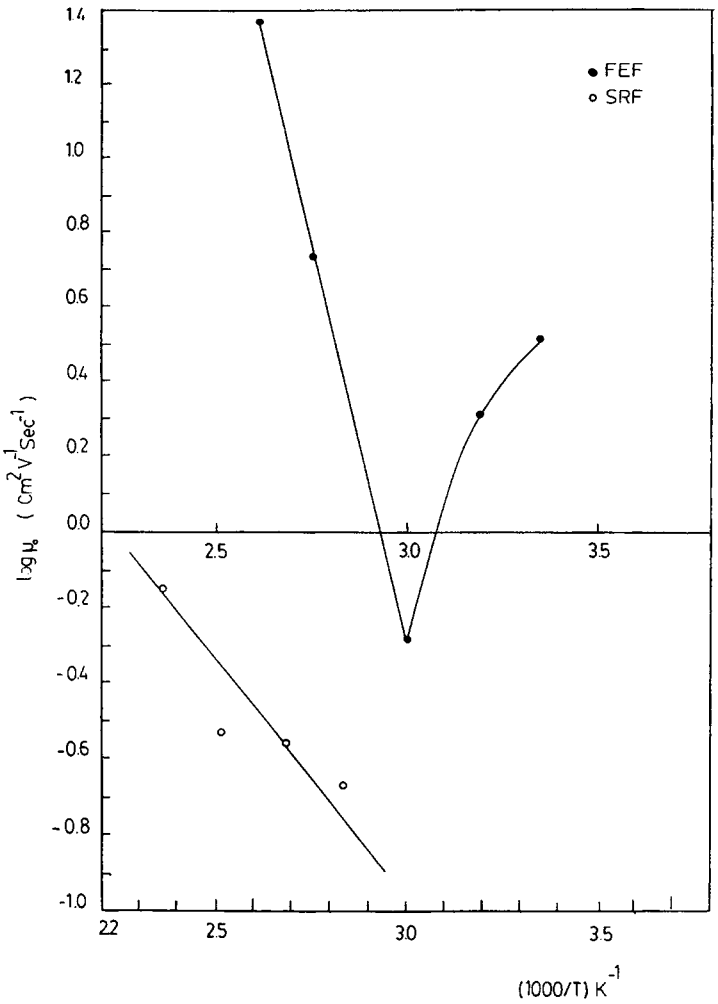

Figure 6 Log $\mu_0 - 1/T$ plot for the FEF and SRF composites.

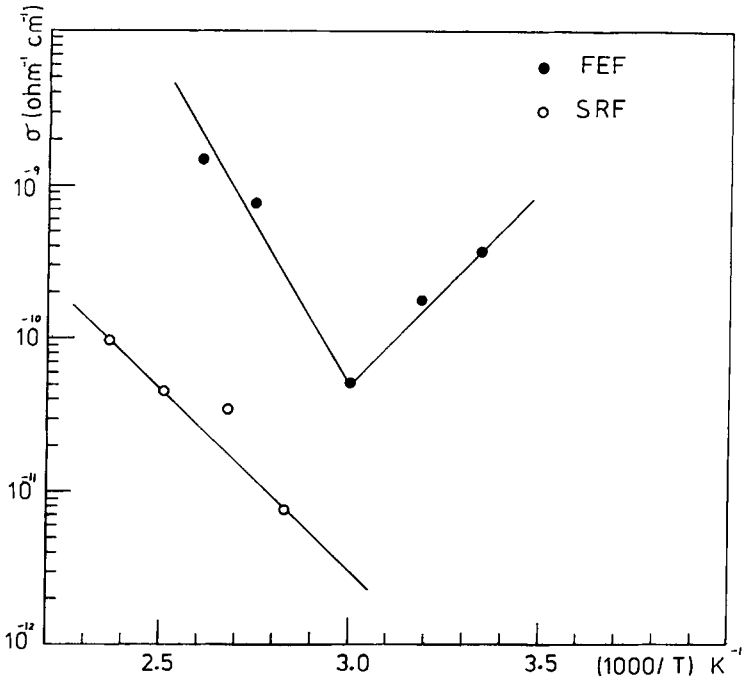

Figure 7 $\sigma - 1/T$ plot on a semilog scale for the FEF and SRF composites (derived from ohmic region of I–V curves).

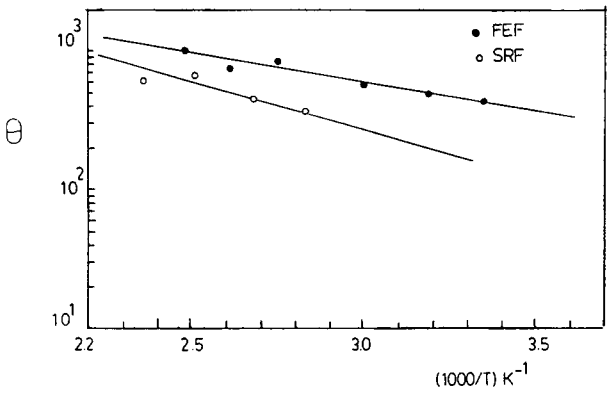

Figure 8 $\theta - 1/T$ plot on a semilog scale for the FEF and SRF composites.

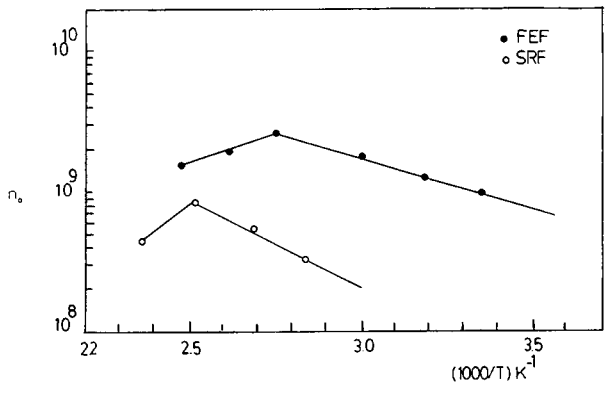

Figure 9 $n_0 - 1/T$ plot on a semilog scale for the FEF and SRF composites.

ing these values in eq. (9), we found that the mobility of the current carrier in a crystalline polymer lies between 0.39 and 0.039 $cm^2\ V^{-1}\ s^{-1}$ at room temperature.

For the SRF composite that is a crystalline polymer containing SRF carbon black as a conducting filler, the free current carrier mobility was found to be 0.21 $cm^2\ V^{-1}\ s^{-1}$ at 353 K as calculated from the trap–square law region. Thus, we found that the carrier mobility in the SRF composite lies between those of a crystalline polymer. This means that the carrier mobility in IIR, which is a crystalline polymer, was not affected by the mixing with SRF carbon black.

For the FEF composite, the free carrier mobility was found to be 3.28 $cm^2\ V^{-1}\ s^{-1}$ at room temperature as calculated from the trap–square law region. We found that this value is higher than those of a crystalline polymer. This means that in FEF composite FEF carbon black not only acts as a conducting filler, but also enhances the carrier mobility. This can be explained as follows: FEF carbon black is a semiactive carbon black that shows a considerable interaction with rubber. The interaction between carbon black and rubber depends mainly upon the surface condition and the surface area of carbon black (55 m^2/gm for FEF). This interaction is of a chemical and physical nature.[21] Chemical interaction leads to the formation of carbon–rubber bonds.[1] These chemical bonds improve the interfacial wetting and adhesion between carbon and rubber.[21] These chemical bonds may also enhance the bandwidth (w) of IIR through the improvement of the overlapping integral (K) where ($w = 4K$).[22] This may lead to higher mobility and explain the disappearance of the reduction in the electrical conductivity at high field that was observed previously for a crystalline polymer containing no conducting filler.[19] Since the electrical conductivity of carbon–polymer composites depend greatly on the surface condition and the surface area of carbon black and the interaction between carbon and polymer depends mainly upon the same parameters, the above interpretation is logical.

SRF carbon black of a surface area 28 m^2/g is a nonactive carbon black, i.e., it shows no considerable interaction with IIR. Therefore, the mobility of the free carrier in the SRF composite lies between those of a crystalline polymer containing no conducting filler.

Comparing Figures 6, 7, and 9, we found that, for the FEF composite, the variation of σ with T follows the variation of μ_0 with T rather than n_0 with T.

It was established that if μ_0 is greater than 1.0

Table III Parameters for FEF Composite at Various Temperatures

Temp (°C)	$\sigma_{measd} \times 10^{10}$ $ohm^{-1}\ cm^{-1}$	$\sigma_{calcd} \times 10^{10}$ $ohm^{-1}\ cm^{-1}$	$\theta \times 10^2$	μ_0 ($cm^2\ V^{-1}\ s^{-1}$)	μ_e ($cm^2\ V^{-1}\ s^{-1}$)	$n_0 \times 10^{-9}$ cm^{-3}	$n_t \times 10^{-10}$ cm^3	E_t (eV)	$N_t \times 10^{-11}$ cm^{-3}
25	3.8	5.2	4.40	3.28	0.14	0.96	2.08	0.09	2.07
40	1.8	4.3	4.90	2.05	0.10	1.30	2.46		2.07
60	0.5	1.5	5.75	0.51	0.03	1.80	2.90		2.40
90	7.8	21	8.23	5.45	0.45	2.43	2.70		1.76
110	15	71	7.54	23.61	1.78	1.9	2.30		1.60

Table IV Parameters for SRF Composite at Different Temperatures

Temp (°C)	$\sigma_{measd} \times 10^{11}$ ohm^{-1} cm^{-1}	$\sigma_{calcd} \times 10^{11}$ ohm^{-1} cm^{-1}	$\theta \times 10^2$	μ_0 (cm^2 V^{-1} s^{-1})	$\mu_e \times 10^2$ (cm^2 V^{-1} s^{-1})	$n_0 \times 10^{-8}$ cm^{-3}	$n_t \times 10^{-10}$ cm^{-3}	E_t (ev)	$N_t \times 10^{-11}$ cm^{-3}
80	0.76	1.1	3.50	0.21	0.74	3.30	0.91	0.14	1.30
100	3.4	2.3	4.50	0.26	1.20	5.60	1.19		0.15
125	4.5	3.6	6.25	0.29	1.80	7.80	1.17		1.17
150	9.5	5.3	5	0.76	3.80	4.40	0.84		1.10

cm^2 V^{-1} s^{-1} and varies with T^{-n} the conduction mechanism is a convertional band model, while if it is less than 1.0 cm^2 V^{-1} s^{-1} and varying as $\exp(-E_\mu/kT)$, where E_μ is the mobility activation energy, the conduction mechanism is the hopping mechanism.[12,13] In the FEF composite, μ_0 is greater than 1.0 cm^2 V^{-1} s^{-1} (3.28 cm^2 V^{-1} s^{-1}) at room temperature and decreases with increasing temperature (see Fig. 6) up to 333 K. Therefore, one can conclude that the conduction mechanism in the FEF composite is a conventional band model up to 333 K. Above 333 K, σ obeys the Arrhenius relation

$$\sigma = \sigma_0 \exp(-E/kT) \qquad (10)$$

where σ_0 is a constant and E is the activation energy. Since μ_0 at the beginning of the transition temperature (333 K) is 0.5 cm^2 V^{-1} s^{-1} and thermally activated (see Fig. 6) with the activation energy (E_μ = 0.85 eV), one can conclude that the conduction mechanism above the transition temperature is the hopping mechanism with the activation energy (E = 0.8 eV) for the FEF composite.

The above discussion for the FEF composite is reasonable because as the temperature increases, the bandwidth decreases and mobility decreases [see eq. (9)] and the transition from the band conduction model to the hopping model is possible at a certain temperature.

For the SRF composite μ_0 and, hence, σ are thermally activated with activation energies E_μ = 0.24 eV and E = 0.48 eV, respectively.

Concerning the reproducibility of the temperature dependence of σ, Figure 10 shows the variation of σ with $1/T$ for other samples of FEF and SRF composites (not those of I–V curves). Comparing Figures 7 and 10, we find that the behavior of σ with $1/T$ is the same for both composites, but there is a slight difference in the conductivity values, and the transition temperature of the FEF composite is shifted toward higher a temperature value (363 K). This is because, in carbon–rubber composites, it is difficult to obtain two samples of the same composite having the same carbon distribution (dispersion). The bending in σ toward a saturation value that was observed for the SRF composite above 373 K may be attributed to the tendency of n_0 to decrease with T above 373 K (Fig. 9).

Finally, the following was concluded:

1. For IIR mixed with 40 phr of FEF carbon black, the conduction mechanism is a conventional band approach followed by the hopping model at a certain temperature.
2. For IIR mixed with 50 phr of SRF carbon black, the conduction mechanism is the hopping model with the activation energy (E = 0.48 eV).

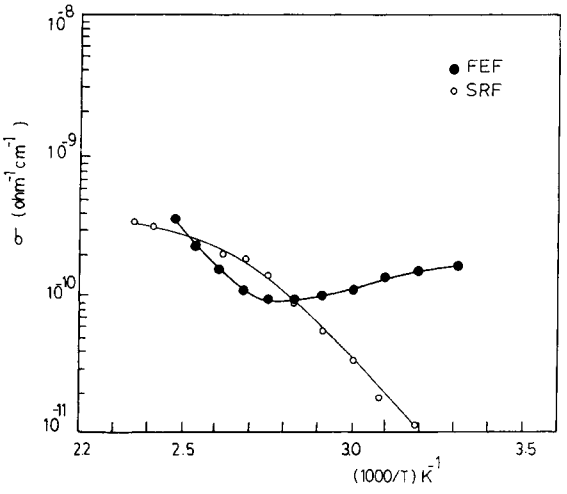

Figure 10 $\sigma - 1/T$ plot on a semilog scale for other samples of FEF and SRF composites.

The author wishes to express his thanks to Prof. A. A. Ghani for helpful discussion.

REFERENCES

1. R. H. Norman, *Conductive Rubbers and Plastics*, Applied Science, London, 1970.
2. F. Bueche, *J. Appl. Phys.*, **43**, 4837 (1972); *J. Appl.*

Phys., **44,** 532 (1973); *J. Polym. Sci. Polym. Phys. Ed.*, **11,** 1319 (1973).
3. J. P. Rebouland and G. Moussalli, *Int. J. Polym. Mater.*, **5,** 133 (1976).
4. R. M. Scarisbrick, *J. Phys. D*, **6,** 2098 (1973).
5. M. Amin, H. H. Hassan, and E. M. Abdel-Bary, *J. Polym. Sci. Polym. Chem. Ed.*, **12,** 2651 (1974).
6. E. M. Abdel-Bary, *J. Polym. Sci. Polym. Chem. Ed.*, **17,** 2163 (1979).
7. A. I. Eatah, A. A. Ghani, and A. A. Hashem, *Angew. Makromol. Chem.*, **165,** 69 (1989).
8. A. A. Hashem, A. A. Ghani, and A. I. Eatah, *J. Appl. Polym. Sci.*, **42,** 1081 (1991).
9. L. K. H. Beek and B. I. C. F. van Pul, *J. Appl. Polym. Sci.*, **6,** 651 (1962).
10. P. Gaillon, J. Reboul, and A. Toureille, *C. R. Acad. Sci. Paris* **272,** 1074 (1971).
11. M. Morton, *Rubber Technology*, van Nostrand Reinhold, New York, 1973, p. 76.
12. D. A. Seanor, *Electrical Properties of Polymers*, Academic Press, New York, London, 1982, p. 34.
13. A. D. Jenkins, *Polymer Science*, North-Holland, Amsterdam, London, 1972, p. 1210.
14. J. Chutia and K. Barua, *J. Phys. D Appl. Phys.*, **13,** L9–13 (1980).
15. M. A. Lampert, *Phys. Rev.*, **103,** 1648 (1956); *Proc. I. R. E.*, **50,** 1781 (1962).
16. A. I. Eatah, K. N. Adel-El-Nour, A. A. Ghani, and A. A. Hashem, *Polym. Degrad. Stab.*, **22,** 91 (1988).
17. S. H. Glarium, *J. Phys. Chem. Solids*, **24,** 1577 (1963).
18. SBP Board of Cansultants and Engineers, Rubber Technology and Manufacture, Small Business Publication, SBP Building 4, 45 Roop Nagar Delhi, 1980.
19. A. A. Shilyaev and L. G. Gindin, *Sov. Phys. Solid State*, **4**(14), 1094 (1972).
20. H. Inokutiand and H. Akamatu, *Electrical Conductivity of Organic Semiconductors* (Russian translation), IL, Moscow, 1963.
21. G. Kraus, *Rubber Chem. Technol.*, **51,** 297 (1978).
22. J. J. O'Dwyer, *The Theory of Electrical Conduction and Breakdown in Solid Dielectrics*, Clarendon Press, Oxford, 1973.

Received May 30, 1991
Accepted September 30, 1991